

Precise Microinjection into Skin Using Hollow Microneedles

Ping M. Wang^{1,2}, Megan Cornwell^{2,3}, James Hill^{2,4} and Mark R. Prausnitz^{1,2}

Hollow needles of micron dimensions have previously been fabricated and envisioned for use with transdermal patches or infusion pumps to achieve painless delivery of drugs to the skin for local and systemic effects without the need for hypodermic needles. However, little work has been carried out to identify methods to effectively use hollow microneedles for drug delivery. To address this need, we inserted hollow, glass microneedles into hairless rat skin *in vivo* and human cadaver skin *in vitro* and then imaged infusion of dye molecules, insulin, polymer microparticles, and cells into the skin by brightfield and fluorescence microscopy. The depth of needle penetration into skin was controlled by inserting needles with a rotary drilling device, which enabled localized injection within the epidermis or dermis with $\pm 60 \mu\text{m}$ resolution. Although small quantities of fluid could be injected after needle insertion into skin, partial retraction of the needle by withdrawing back 100–300 μm or vibrating the microneedle array dramatically increased infusion flow rate. We conclude that hollow microneedles can be used for precise microinjection into skin, especially when a single needle is inserted by rotary drilling and then retracted part way before infusion or a microneedle array is inserted by mechanical vibration.

Journal of Investigative Dermatology (2006) **126**, 1080–1087. doi:10.1038/sj.jid.5700150; published online 16 February 2006

INTRODUCTION

Clinical and research applications require delivery of compounds into skin for local dermatological effects or systemic effects after absorption into the bloodstream via dermal capillaries. Drugs and other compounds are usually delivered to the skin by passive mechanisms, where a topical formulation or patch is applied to the skin surface and the drug compound diffuses into the skin across stratum corneum.

As the stratum corneum's barrier properties severely limit passive delivery of most drugs, and especially macromolecules and microparticles, intradermal injection using a hypodermic needle is an effective alternative. However, the pain and inconvenience of intradermal injection generally precludes self-administration by patients or other uses outside the clinic or laboratory. Moreover, the relatively large size of hypodermic needles and their relatively poorly controlled manual insertion into skin makes targeted delivery to sites within skin difficult.

Alternative methods of delivery into skin have been developed to more effectively drive drugs across stratum

corneum without the use of a needle (Prausnitz *et al.*, 2004; Bronaugh and Maibach, 2005). Iontophoresis, electroporation, ultrasound, thermal ablation, particle bombardment, and other methods have received considerable interest, but have yet to make significant clinical impact. Moreover, other than the possible exception of particle bombardment (Burkoth *et al.*, 1999), these methods do not address intracutaneous targeting.

Recently, arrays of needles measuring just microns in dimensions have been fabricated by adapting techniques borrowed from the microelectronics industry (McAllister *et al.*, 2000; Prausnitz, 2004; Reed and Lye, 2004). These microneedles have been shown to increase skin permeability to drugs and particles by orders of magnitude *in vitro* (McAllister *et al.*, 2003; Chabri *et al.*, 2004). *In vivo* animal studies have shown delivery of insulin (Gardeniers *et al.*, 2003; Martanto *et al.*, 2004; Davis *et al.*, 2005), oligonucleotides (Lin *et al.*, 2001), human growth hormone (Cormier and Daddona, 2003), and desmopressin (Cormier *et al.*, 2004), as well as ovalbumin (Matriano *et al.*, 2002), DNA (Mikszta *et al.*, 2002) and anthrax (Mikszta *et al.*, 2005) vaccines. Human studies demonstrated that microneedles can be inserted painlessly into the skin (Kaushik *et al.*, 2001; Mikszta *et al.*, 2002).

Although significant attention has been given to fabrication of both solid and hollow microneedles, most drug delivery studies have employed just solid microneedles used either to pierce holes in the skin as a pretreatment before application of a transdermal patch or coated with drug that dissolves off the needles upon insertion into the skin. Hollow microneedles have been shown to deliver pharmacologically

¹School of Chemical and Biomolecular Engineering, Atlanta, Georgia, USA;

²Institute for Bioengineering and Bioscience, Georgia Institute of Technology, Atlanta, Georgia, USA; ³Agnes Scott College, Decatur, Georgia, USA and

⁴Morehouse College, Atlanta, Georgia, USA

Correspondence: Dr Mark R. Prausnitz, School of Chemical and Biomolecular Engineering, Georgia Institute of Technology, 311 Ferst Drive, Atlanta, Georgia 30332-0100, USA. E-mail: prausnitz@gatech.edu

Abbreviations: H&E, hematoxylin and eosin; PBS, phosphate-buffered saline
Received 9 August 2005; revised 7 October 2005; accepted 2 November 2005; published online 16 February 2006

active insulin to diabetic rats (Gardeniers *et al.*, 2003; McAllister *et al.*, 2003). In these studies, only systemic effects were measured, whereas delivery and transport within the skin were not addressed.

Hollow microneedles have received less attention in part because they are harder to use. Hollow microneedles are inherently weaker than solid microneedles and therefore have additional constraints on needle design and insertion methods (Davis *et al.*, 2004). Placement of the bore opening at the needle tip reduces needle tip sharpness and makes insertion into skin more difficult. Flow through the bore of hollow microneedles is also difficult to achieve, probably owing to the resistance to flow provided by dense dermal tissue beneath the microneedle tip and blockage owing to possible tissue coring within the needle bore (Martanto *et al.*, 2006).

Given these challenges, the goal of this study was to develop a microneedle design and insertion protocol that pierces microneedles into the skin in a controlled manner and allows precise microinjection at controlled locations within the skin and at controlled rates of fluid flow. Spatial targeting of microinjection is desirable for clinical applications that seek to target vaccines to epidermal Langerhans cells, systemic drugs to the superficial dermal capillary bed, or local drugs to the deeper dermis to minimize systemic absorption. Spatially targeted delivery is also desirable for research applications that seek to selectively deliver macromolecules, particles used as drug carriers, or possibly cells to different regions of the skin.

As a model for microfabricated, hollow, metal microneedles suitable for mass production, this study used hollow, glass microneedles, which are easily fabricated for small-scale research purposes and have a transparent wall that facilitates viewing inside the lumen. Such micropipettes are extensively used in cellular physiology, genetics, and neurophysiology to microinject substances into cells, extract fluid, or record electrical activity for a variety of different experimental purposes (Brown and Flaming, 1987). By using this widely available method of making microneedles, researchers without access to sophisticated microfabrication facilities can reproduce our results for their own applications, whereas those interested to develop microfabricated devices can be guided by microneedle design and applications evaluated in this study.

RESULTS

Controlled microneedle insertion and injection into skin

To insert microneedles in a controlled manner into the skin of hairless rats *in vivo* and human cadaver skin *in vitro*, we developed a hand-operated, rotary penetration device that drilled individual microneedles into the skin to a predetermined depth regulated by the number of turns of the device. This rotary drilling approach was designed to reduce the force of insertion into skin, based on the expectation that drilling insertion should cause less skin deformation than direct penetration. After insertion in this manner, the glass microneedles were found to be mechanically robust; needles could be inserted into the skin repeatedly (i.e., > 10

times) without damage to the needle, as determined by microscopy.

The hole punctured in the skin by microneedles could be viewed after inserting and removing the microneedle. When viewed *in situ* from the skin surface of a hairless rat, holes with diameters ranging from 100 to 300 μm were imaged by microscopy (e.g., Figure 1a). These holes on the surface on hairless rat skin disappeared within 10–20 minutes *in vivo*, based on visual observation through a stereomicroscope. Only mild, localized erythema was observed immediately after microneedle treatment, which disappeared within minutes. These kinetics are similar to observations made in human subjects (Kaushik *et al.*, 2001). Microneedle insertion and injection caused no significant complications in the animals.

Histological sectioning of skin *in vitro* shows the shape and depth of needle penetration pathways. Figure 1b shows a series of sequential cross-sectional images taken parallel to the skin surface, which gives an indication of the pathway geometry at different depths in the skin. Figure 1c shows a series of sequential cross-sectional images taken perpendicular to the skin surface and stained with tissue-marking dye injected by the microneedle. These images show a tapered pathway with a geometry similar to that of the microneedle.

The rotary drilling method was designed not only to reduce the force required for penetration into skin but also to facilitate microinjection at precise locations within the skin. Figure 2a demonstrates this, where injections were made at three different predetermined depths within the dermis of hairless rats *in vivo*. In this case, injection depth ranged from just below the dermal–epidermal junction to the mid-dermis. Injection in this region may be of interest to target delivery to the rich capillary bed found in the superficial dermis for uptake and systemic distribution in the bloodstream. As shown in Figure 2b, even shallower skin

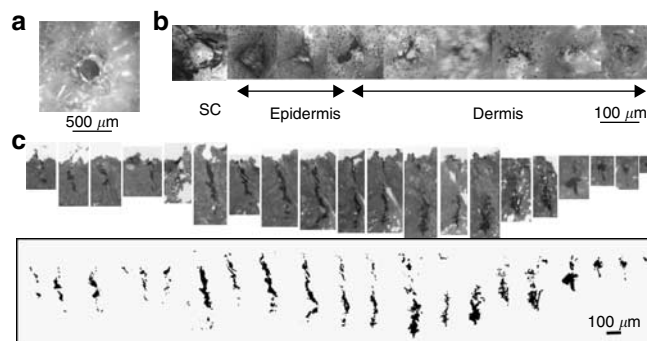


Figure 1. Imaging of microneedle track pathways when inserted into hairless rat skin *in vivo*. (a) Hole in skin imaged *in situ* on the skin surface of an anesthetized hairless rat after insertion and removal of a microneedle. (b) Sequence of H&E-stained histological sections taken parallel to the surface of *in vitro* hairless rat skin surface after piercing with a microneedle. (c) Sequence of H&E-stained histological sections taken perpendicular to the surface of *in vitro* hairless rat skin after piercing with a microneedle and injecting tissue-marking dye. The lower set of images shows areas of dye staining determined by image processing of the upper set of histological sections.

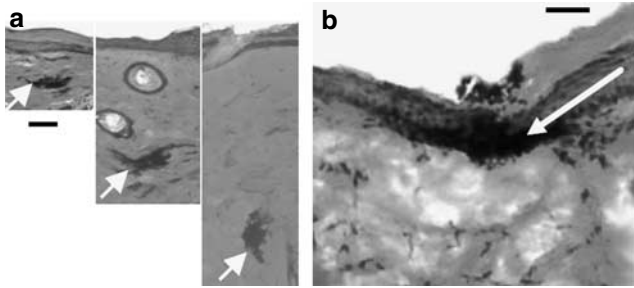


Figure 2. Highly targeted microinjection at various depths within the dermis and epidermis. H&E-stained histological sections of hairless rat skin microinjected *in vivo* with tissue-marking dye at three controlled depths (arrows) in (a, bar = 100 μm) the dermis and (b, bar = 50 μm) localized within the epidermis.

penetration and injection can target delivery to the epidermis, which may be useful for various dermatological therapies, as well as for vaccine delivery to Langerhans dendritic cells found in the epidermis.

To quantify the precision and reproducibility of targeted insertion, microneedles were inserted into the back skin on hairless rats *in vivo* at six predetermined depths over the range 150–770 μm deep (corresponding to 180–1,080° rotation of the insertion device). Based on three replicates at each condition, the average standard error was $\pm 60 \mu\text{m}$ on an absolute basis and $\pm 16\%$ on a percent basis. The exact relationship between rotation of the insertion device and depth of penetration into the skin is a complex function of skin mechanical properties, needle geometry, and other factors. While we were able to insert microneedles to desired depths under the controlled and reproducible conditions used in this study, controlled insertion at different skin sites, using different needle geometries, or other possible variations will require re-calibration.

Microneedle retraction to increase flow rate into skin

Data presented so far have marked the sites and tracks of needle penetration, but have not addressed flow of significant amounts of fluid into the skin. To address this scenario, the process of microinjection was imaged *in situ* by piercing hairless rat cadaver skin from above with a microneedle and viewing flow of fluorescent solution into the skin from below in real time. Insertion of a microneedle in this manner showed local injection of fluorescent solution, consistent with imaging results above, but flow into skin was slow (Figure 3a).

We hypothesized that flow might be limited owing to the inability of fluid to flow out of the needle and into the dense dermal tissue surrounding the needle tip that was compressed during needle insertion. Alternatively, dermal tissue might have penetrated into the needle bore owing to tissue coring. In either event, pulling the needle part way back could facilitate microinjection by relieving tissue compression and/or withdrawing cored tissue from the needle bore. Consistent with this hypothesis, we found that slightly retracting the needle had a large effect on flow into skin (Figure 3b). Within a few seconds, the field of view imaged by the microscope

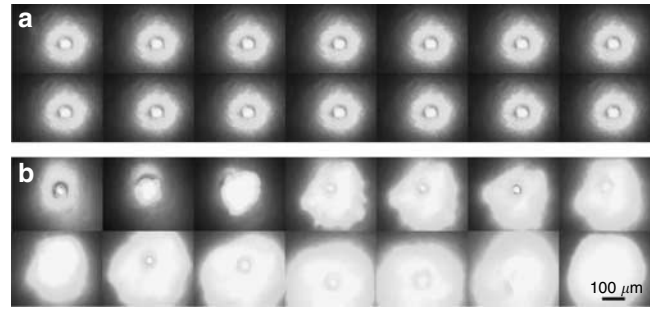


Figure 3. Partial microneedle retraction after insertion into skin dramatically increases injection flow rate. Fluorescence micrographs of calcein microinjection into hairless rat skin *in vitro* at 10 psi. Images were recorded every 2 seconds using real-time microscopy. In (a), the microneedle was inserted to a depth of approximately 800 μm and flow was initiated at the first frame. No significant change in fluorescence was observed, corresponding to little or no injection into the skin. In (b), the microneedle was initially inserted to the same depth, but was then retracted approximately 200 μm before initiating flow at the first frame. Large increases in fluorescence were observed, corresponding to rapid infusion into the skin.

was filled with fluorescent solution. Macroscopic examination of the tissue afterwards showed fluorescent solution infusion over much larger areas, depending on the duration of microinfusion (data not shown). Absolute quantification of flow rates in this case was difficult. However, measurements carried out in human cadaver skin using a similar apparatus in a separate study measured flow rates of 21–1,130 $\mu\text{l}/\text{hour}$ through individual microneedles, which increased strongly with microneedle retraction (Martanto *et al.*, 2006).

Microinjection of insulin, microparticles, and cells

Macromolecules, microparticles, and cells can also be delivered using microneedles. To demonstrate delivery of a bioactive macromolecule, insulin solution was microinjected into hairless rat skin *in vitro*. Using fluorescently labeled insulin, the drug was observed to distribute throughout the dermis (Figure 4). Although the injection was at a specific location within the dermis, the large volume of fluid injected in this case spread throughout the dermis. Careful examination shows that there is only weak fluorescence from within the epidermis, suggesting that insulin had difficulty crossing the dermal-epidermal junction and remained within the dermis. This contrasts with microinjection of calcein, which fluoresced more uniformly in both dermis and epidermis (data not shown).

As a companion experiment, insulin was microinjected into the skin of diabetic hairless rats *in vivo* and blood glucose concentration was monitored over time. Microinjection was carried out via microneedle insertion to a depth of 500–800 μm and infusing for 30 minutes. Over a 4.5-hour monitoring period after infusion, blood glucose level dropped and then plateaued at approximately 25% below pre-treatment values (Figure 5). This drop was significantly lower than blood glucose levels in a negative control group microinjected with saline ($P < 0.05$). The volume of insulin solution microinjected into diabetic rat skin was $5 \pm 1 \mu\text{l}$ over the 30-minute infusion period.

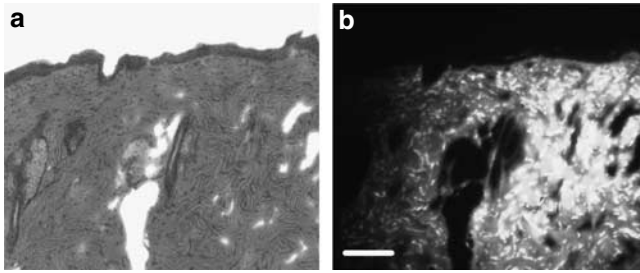


Figure 4. Microinjection of insulin into skin. Hairless rat skin was microinjected *in vivo* with FITC-insulin. Histological sections are shown using (a) brightfield microscopy with H&E staining and (b) fluorescence microscopy showing injection and distribution of insulin in the skin. Bar = 100 μm .

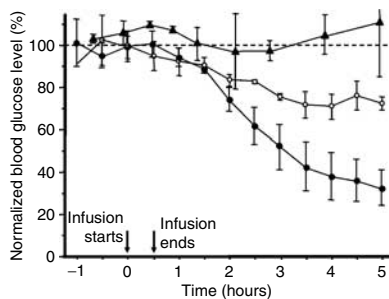


Figure 5. Insulin microinjection modulates blood glucose levels in diabetic rats. Changes in blood glucose level in diabetic hairless rats before, during, and after a 30-minute infusion from a microneedle: (▲) infusion of saline as a negative control ($n=4$), (○) infusion of insulin for microneedle inserted 800 μm ($n=3$), (●) infusion of insulin solution using microneedle inserted 800 μm and then retracted $\sim 200 \mu\text{m}$ ($n=4$). Data expressed as mean \pm SEM.

Recognizing that needle retraction can increase microinfusion, the insulin delivery experiment was repeated by inserting microneedles to the same initial depth in the skin and then retracting by $\sim 200 \mu\text{m}$ back toward the skin surface. As before, blood glucose level dropped after microinfusion, but this time dropped approximately 70% below pre-treatment values (Figure 5), which was a significantly greater effect than that caused by saline infusion or insulin infusion without retraction ($P < 0.05$). The volume of insulin solution microinjected into diabetic rat skin after needle retraction was $29 \pm 12 \mu\text{l}$ over the 30-minute infusion period. Microinfusion in this manner may find applications for continuous or intermittent drug delivery from an indwelling microneedle, which could provide an alternative to the macroscopic catheters currently used for insulin pump therapy (Lenhard and Reeves, 2001).

Although microneedles are small, their microns dimensions should be large enough to inject cells, which may be of interest for tissue engineering, stem cells, and other cell-based therapies, and microparticles, which may be of interest for controlled release drug delivery. Initial experiments to test the effects of shear stress experienced by cells during infusion through microneedles in the absence of skin flowed suspensions of newborn mouse dermal fibroblasts (provided courtesy of Dr Kurt Stenn, Aderans Research Institute,

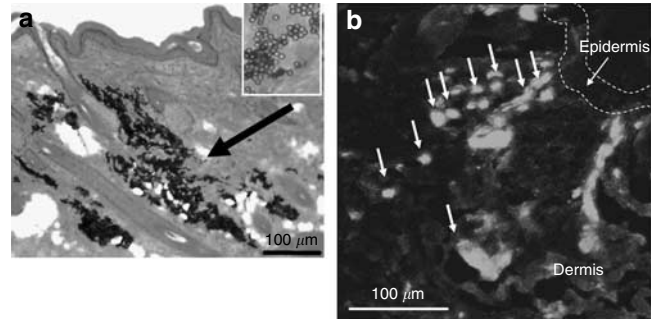


Figure 6. Microinjection of polymeric particles and cells into hairless rat skin *in vivo*. (a) Brightfield micrograph of H&E-stained histological section of *in vitro* hairless rat skin after microinjection with 2.8- μm polymeric microspheres. Inset shows magnified view of microspheres in skin. (b) Fluorescence micrograph of histological section of hairless rat skin after *in vivo* microinjection of fluorescence-labeled Caco-2 human intestinal epithelial cells.

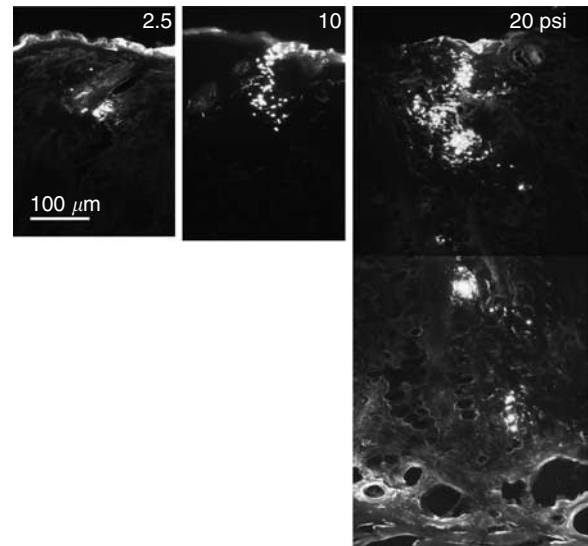


Figure 7. Microinjection of polymeric particles at different pressures. Fluorescence micrographs of histological sections after microinjection of 2.5- μm fluorescent microspheres into hairless rat skin *in vivo* under pressures ranging from 2.5 to 20 psi via the same needle and loading for the same time periods. The volume and depth of injection increased with increasing pressure.

Philadelphia, PA) through microneedles at rates up to 100 $\mu\text{l}/\text{second}$ and showed no significant loss of cell viability. Follow-on experiments demonstrated microinjection of 2.8- μm polymeric microspheres and Caco-2 human intestinal epithelial cells into rat skin *in vivo* (Figure 6). At smaller injection pressures, microparticles tended to collect near the needle tip, whereas at larger pressures they filled the needle track and at still larger pressures they penetrated deeper into the skin (Figure 7).

Microneedle vibration for injection using microneedle arrays
Although drilling and retraction are effective to control injection using single microneedles, drilling may be difficult

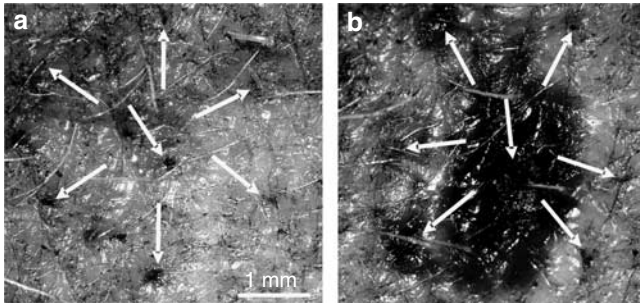


Figure 8. Vibration of microneedle arrays during insertion increases microinjection. Seven-needle arrays of microneedles were inserted into hairless rat skin *in vivo* and used to inject tissue-marking dye. (a) Intracutaneous staining imaged *in situ* at the skin surface shows little microinjection when the needle array was inserted without vibration for 10 minutes. (b) Much more dye was injected when the needle array was vibrated during and for 1 minute after insertion.

to implement with multi-needle arrays. As an alternative, microneedle arrays were inserted into skin using vibration (i.e., without rotary drilling or retraction), which also was effective to facilitate microinjection. As shown in Figure 8, injection from a seven-needle array into hairless rat skin without vibration introduced very little dye into the skin, whereas injection after insertion using vibration delivered much more. Although this demonstrates the feasibility of a vibration-based approach, additional study is needed to better optimize and evaluate this method.

DISCUSSION

This study introduced the idea of inserting microneedles into skin using a rotary drilling device to precisely deliver drug solutions, solid particles, and cells at controlled depths into epidermis and dermis. This study also demonstrated for the first time that partial needle retraction after insertion into the skin or insertion and infusion during mechanical vibration can dramatically increase microinjection flow rate into the skin.

Precise microinjection into skin

The ability to precisely inject fluids, macromolecules, particles, and cells into skin at controlled depths and controlled amounts is important to a variety of applications. Dermatological treatments could benefit from intracutaneous delivery with minimal tissue trauma. The ability to target specific layers of the skin could also increase treatment efficacy. Vaccine delivery to the skin has previously been shown to elicit stronger immune responses than injection into deeper tissue (Glenn *et al.*, 2003). Delivery to the epidermis could further target the Langerhans cells believed to be responsible for the enhanced immune response; alternatively, dermal dendritic cells could be targeted by controlled injection into the dermis. Systemic delivery could also benefit from infusion to the dermal capillary bed for rapid uptake and distribution. Researchers might also find precise microinjection into skin useful to develop clinical treatments, as well as to address mechanistic questions requiring targeting specific cells or layers of skin.

The hollow, glass microneedles used in this study have strengths and weaknesses. As a laboratory tool, glass microneedles offer the advantage of being simple and inexpensive to make using widely available techniques and equipment. Glass microneedle strength was increased by heating the tip to smooth and thicken the wall. Handling was facilitated by placing needles within a hand-operated drilling insertion device.

Despite the versatility of microneedles made from glass pipettes in the laboratory, clinical applications would benefit from microneedles made from different materials and by different methods. To address this need, the literature contains many studies showing how to make microneedles out of other materials, such as metal, using microfabrication techniques that could be scaled up for mass production at disposable cost (McAllister *et al.*, 2000; Prausnitz, 2004; Reed and Lye, 2004). We performed a preliminary study to mold microneedles for mass production, as discussed in Materials and Methods.

Despite impressive fabrication advances, the literature has offered relatively little information about how to use these microneedles for medical and other applications. This study found that drilling insertion and partial needle retraction can be used to make microneedle injection more controlled and effective. Drilling was advantageous because it reduced skin deformation during needle insertion and thereby provided more control of insertion depth. Although reduced, there was still some skin deformation during insertion, so that the insertion depth into skin was only proportional, but not equal, to the microneedle displacement distance during insertion. Because insertion of multi-needle arrays may be difficult using rotary drilling, we found that microneedle arrays could be effectively inserted using vibration. In a related study, the insertion force of microneedles was also reduced using vibration (Yang and Zahn, 2004)

Partial needle retraction was advantageous because it increased the flow rate during infusion by many fold. This indicates that microneedle insertion may compress skin tissue to form a dense barrier that blocks fluid flow and dispersion at the microneedle tip. Retracting the microneedle to create a space for fluid flow and using a beveled microneedle with a bore opening on the side of the microneedle tip may avoid the need to force fluid into the compressed tissue layer and thereby increase the infusion rate.

Imaging methods

Each of the three methods used to image injection have strengths and weaknesses. Determining injection volume by measuring the dyed area shown in skin section images using the magic wand tool of Adobe Photoshop (version 5.0; Adobe Systems, San Jose, CA) for histological slide imaging or based on a specified threshold gray level for microtome imaging assumed that the injected dye was uniformly dispersed in the skin tissue and there was no loss of dye during the histological slice preparation. Although microtome imaging reduced the chance of artifact by avoiding preparation of histological slides, selecting the gray level threshold strongly

influenced the area calculation and thereby introduced uncertainty.

Real-time, *in situ* imaging on the microscope stage further reduces the chance of artifact owing to sample handling and also provides a fluorescence measurement that is a direct measure of volume rather than area from a cross-section of tissue. This volume measurement, however, is only accurate for a limited thickness of tissue within the focal range of the microscope objective. Real-time imaging also facilitates studying the dynamics of microinjection, which makes this approach especially attractive.

Conclusions

Hollow, glass microneedles were fabricated using a method readily reproduced in biomedical laboratories to serve as a model for microneedles mass produced by microfabrication. Using a rotary drilling method, microneedles were inserted into the skin at controlled depths within the epidermis or dermis. By partially retracting microneedles after insertion, flow rate into the skin was dramatically increased for delivery of small dye molecules, insulin, polymer particles, and cells. This represents the first study to carefully examine needle insertion and infusion parameters to enable controlled and targeted intracutaneous delivery using hollow microneedles. The results suggest applications in dermatological research, as well as minimally invasive clinical applications for local and systemic delivery of drugs, vaccines, particles, and cells.

MATERIALS AND METHODS

Microneedle fabrication

Glass microneedles were made using conventional drawn glass micropipette techniques (Brown and Flaming, 1987). Microneedles were prepared by pulling glass capillary tubing (OD 1.5 mm, ID 1.1 mm, B150-110-10, borosilicate glass; Sutter Instrument, Novato, CA) with a puller (P97; Sutter Instrument) that reproducibly pulled needles with desired geometries according to programmable parameters. Blunt glass microneedles were fabricated with outer radii at the tip of 15–40 μm and cone angles of 20–30° (Figure 9a). We further used a needle beveller (BV-10; Sutter Instrument) to grind the needle tip, which was then briefly heated to smooth the surface and produce a beveled tip with a side-opening bore having an oval geometry with a short ellipsoidal axis of 60–110 μm and a long ellipsoidal axis of 80–160 μm (Figure 9b). Microneedles were cleaned sequentially with a chromic acid cleaning solution (Klean AR; Mallinckrodt, Phillipsburg, NJ), water, and acetone.

To increase their strength, microneedle tips were quickly heated using a Bunsen burner for 1–2 seconds to smooth and thicken the needle wall at the tip. Microneedles were also sometimes assembled into seven-needle bundles using epoxy resin (Polyoxy 1010; Polytek, Easton, PA) to form multi-needle arrays (Figure 10a and b). Microneedle geometry was imaged and measured by microscopy. The occasional microneedles that were misformed or contaminated with debris were discarded.

To demonstrate polymer molding of microneedles for inexpensive mass production, polymer microneedles were fabricated by first making a mold out of polydimethylsiloxane (Sylgard 184; Dow Corning, Midland, MI) from a master array of glass microneedles and then using the mold to make replicate arrays of polymer

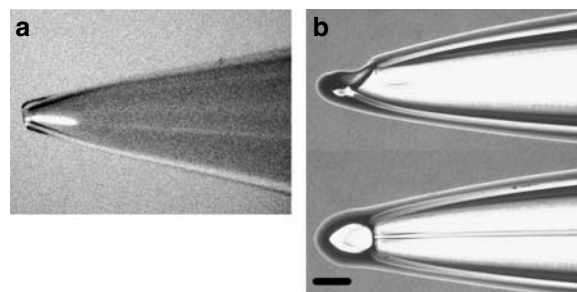


Figure 9. Hollow, glass microneedles used for microinjection. (a) Micro-needle with a bore opening at a blunt tip. (b) Microneedle with a side-opening bore at a beveled tip. Bar = 100 μm .

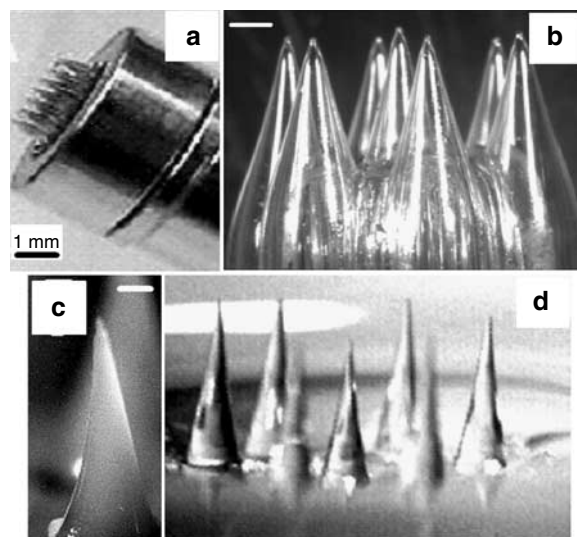


Figure 10. Images of multi-needle glass and polymer microneedle arrays. (a, b) Glass microneedles assembled into an array using epoxy. (c) Polyglycolide polymer microneedle and (d) poly-lactide-co-glycolide polymer microneedle array molded from glass microneedle masters. Bars = 100 μm .

microneedles by casting with poly-glycolide or poly-lactide-co-glycolide (Absorbable Polymers International, Pelham, AL; Park et al., 2005; Figure 10c and d).

Skin models

The *in vitro* skin model was full-thickness human cadaver skin, which was obtained from the Emory University Body Donor Program with approval from the Georgia Institute of Technology and Emory University Institutional Review Boards and used according to the Declaration of Helsinki Principles. Skin samples were stored at -70°C and thawed to room temperature before use. The *in vivo* skin model was healthy, anesthetized, adult, male, Sprague–Dawley hairless rats (weighing 280–410 g; Charles River Laboratories, Wilmington, MA) handled with approval from the Georgia Institute of Technology Institutional Animal Care and Use Committee. For short experiments (< 1 hour), animals were anesthetized by intraperitoneal injection of pentobarbital sodium (60 mg/kg). Additional anesthesia was given according to the animals' depth of anesthesia determined by pedal reflex. At the end of experiments, animals were euthanized with intraperitoneal injection of beuthanasia (390 mg pentobarbital sodium + 50 mg phenytoin sodium/ml, 1 ml/10 lb body

weight). Experimental skin specimens were harvested *post mortem* for histological analysis.

To test the ability of microneedles to deliver insulin to lower blood glucose levels in diabetic animals, we created diabetic rat models as described previously (Martanto *et al.*, 2004). In brief, hairless rats were injected intravenously through the tail vein with 100 mg/kg streptozotocin (Sigma, Milwaukee, WI), which destroyed their pancreatic islet cells (Haughton *et al.*, 1999). Induction of diabetes was verified by measuring blood glucose levels of 350–500 mg/dl (Accu-chek Compact blood glucose meter; Roche Diagnostics, Basel, Switzerland). During insulin delivery experiments, rats were anesthetized by intraperitoneal injection of urethane (200 mg/ml in phosphate-buffered saline (PBS), 1.3 g/kg; Sigma), which provided deep anesthesia for many hours.

Microinjection into skin

Single, hollow, glass microneedles were inserted into the back skin of anesthetized rats placed in a prone position or into human cadaver skin ($2 \times 2 \text{ cm}^2$) placed on a x-y stage. Compounds delivered included blue tissue-marking dye in PBS (20% (v/v); Shandon, Pittsburgh, PA), green fluorescent calcein in PBS (10 μM –10 mM; Molecular Probes, Eugene, OR), clinical insulin solution (100 U/ml; Humulin R, Eli Lilly, Indianapolis, IN), FITC-labeled insulin in PBS (1 mg/ml; Sigma), polymeric microparticles in PBS (2.8 μm diameter, ~2 mg/ml, Epoxy beads M-270 (DynaL Biotech, Brown Deer, WI) or 2.5 μm diameter, 1–2% solids, carboxylate-modified FluoSpheres, yellow-green fluorescent (Molecular Probes)), or Caco-2 intestinal epithelial cells ($3\text{--}5 \times 10^6$ cells/ml; American Type Culture Collection, Manassas, VA) labeled with a fluorescent dye (Hoechst 33258; Molecular Probes).

Microneedles were first filled from the distal end with the above solutions or suspensions using a conventional hypodermic needle (25–31 G; Becton Dickinson, Franklin Lakes, NJ); a thin filament manufactured inside the microneedle lumen enhanced liquid flow to the proximal/tip end of the microneedle and displace air bubbles. Microneedles were connected via tubing to a cylinder of compressed CO_2 , which drove microinfusion at regulated pressures of 5–20 psi for delivery durations of 5–30 minutes.

Microneedles were mounted in a rotary drilling device, which controlled axial translation of the microneedle tip with $\pm 10 \mu\text{m}$ accuracy during drilling into the skin. Device calibration by microscopy determined that every 360° rotation of the drilling device moved the microneedle tip 1,200 μm in its axial direction. However, owing to skin deformation during insertion, microneedle insertion depth into the skin was only ~800 μm under the conditions used in this study, as determined by subsequent histological examination of skin samples. The amount of this deformation was limited not only by the drilling method of insertion, but also by pressing the convex base of the insertion device firmly against the skin surface, which held the skin in place. Before conducting *in vivo* experiments, the insertion device was sterilized by autoclave (AMSCO Scientific Series 3021-S, Erie, PA).

Because it is difficult to insert multi-needle arrays by rotary drilling, microneedle arrays were inserted using a device that vibrated the needle during insertion and injection into skin. The vibration motor operated at a vibration frequency of 24 Hz with an amplitude of 100 μm parallel to the needle axis. These frequency and displacement values were selected based on the convenient

availability of a motor with these specifications and have not been optimized. Note that although the oscillatory vibration amplitude during manual insertion was 100 μm , needles were inserted to a net displacement much deeper.

Histological preparation

After microinfusion experiments, skin samples were harvested from the human cadaver skin or animals *post mortem* and embedded in optimal cutting temperature compound (Tissue-Tek, Sakura Finetek, Torrance, CA) within an embedding mold cup. After rapidly freezing in liquid nitrogen, skin samples were sectioned into 10- to 14- μm thick slices using a cryostat microtome (HM 560; Microm International, Richard-Allan Scientific, Kalamazoo, MI). The cryosection slides were stained with hematoxylin and eosin (H&E) using an autostainer (XL, Leica, Nussloch, Germany).

Microscopic imaging

Imaging of holes on the skin surface and within the skin made by microneedles as well as imaging of fluorescently tagged compounds injected into the skin was performed using either a stereoscopic (SZX12; Olympus, Melville, NY) or an inverted fluorescence microscope (IX 70; Olympus) with a digital camera (Spot RT Slider camera, Model 231; Diagnostic Instruments, Sterling Heights, MI). Images were analyzed using image analysis software (Image Pro Plus, version 4.5; Media Cybernetics, Silver Spring, MD). The volume of injected liquid was imaged in the skin for quantitative analysis using one of three different methods.

The first method was derived from a technique developed to quantify the distribution volume after injection into solid tumors (McGuire and Yuan, 2001). In brief, immediately after microinjection of a blue-green tissue-marking dye solution, skin specimens were frozen in liquid nitrogen and sectioned using a cryostat microtome. The skin slices were imaged by digital microscopy to determine the area stained by the dye. Multiplying this area by the skin section thickness provided a volume. Summing the volumes from all skin sections containing dye yielded the total injected volume.

For the second method, we positioned a mini-video camera at the microtome stage oriented perpendicularly to the sectioning surface of the skin specimen (Figure 11a). Eliminating the time-consuming preparation and imaging of histological slides, as well as the possible loss during the slide preparation of dye delivered into the skin samples, we instead used the video camera (with a resolution of 640×480 pixels) to directly image each sectioned skin slice on the microtome. The images were stored in a computer for further analysis and the skin sections were discarded. The total injected volume was calculated as described above, based on the dyed area and skin section thickness.

During microtome imaging, illumination of the skin specimen was kept constant and the video camera was not moved. To account for different lighting conditions during imaging on the microtome and imaging histological slides, the gray threshold that determined the area of skin considered stained with dye by microtome imaging was selected to yield, on average, the same area acquired by histological imaging.

As a third method, we imaged microinfusion into skin *in situ* in real time. A microneedle filled with fluorescent dye solution of calcein was rotary drilled 500–1,000 μm into a piece of skin (1 cm^2) placed with the stratum corneum side facing up on a glass slide

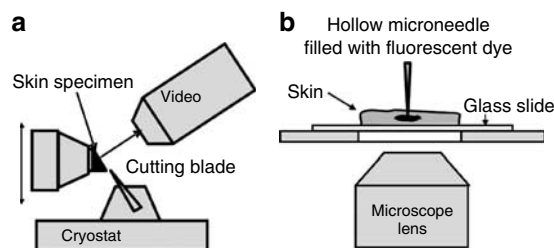


Figure 11. Microscopic methods to image microinjection into skin.

(a) Scheme of the direct-imaging method using a video-microscopy system focused on a cryostat microtome to image the dyed area in each skin cross-section. (b) Scheme of the *in situ* imaging of transdermal microinjection in real time using skin placed on the stage of an inverted microscope.

mounted on the stage of an inverted microscope in a darkened room (Figure 11b). The microscope was focused on the tip of the microneedle and a time series of images was collected every 2 seconds while infusing calcein solution at a pressure of 10 psi.

The relative infusion rate over time was determined by assuming that fluorescence measured in the images was proportional to the injected volume. To express the injected volume on an absolute basis, we determined the total injected liquid volume by measuring the change in weight of the liquid-filled microneedle before and after the injection assuming a liquid density of 1 g/ml using a balance with a sensitivity of ± 0.1 mg.

Statistical analysis

All data are presented as mean \pm standard error of the mean. Student's *t*-test was used to assess statistically significant differences. Comparisons between group means were carried out using analysis of variance. Mean values were considered significantly different if $P < 0.05$. An unpaired *t*-test was used to determine the significance of the differences of blood glucose levels caused by microinjection of insulin and saline in different animals. All statistical analyses were performed using Statview (SAS Institute, Cary, NC).

CONFLICT OF INTEREST

The authors state no conflict of interest.

ACKNOWLEDGMENTS

We thank Esi Ghartey-Tagoe for preparation of fluorescent-labeled Caco-2 cells, Tracy Couse for histological assistance, and Cherry Forkey and Kelly Winn for animal handling assistance. This work was supported in part by the American Diabetes Association, National Institutes of Health, and Aderans Research Institute. MRP is the Emerson-Lewis Faculty Fellow at Georgia Tech and is a member of the Georgia Tech Center for Drug Design, Development and Delivery. MC and JH were supported by the Undergraduate Research Scholars program of the Georgia Tech-Emory Center for the Engineering of Living Tissues.

REFERENCES

- Bronaugh RL, Maibach HI (eds.) (2005) *Percutaneous absorption*. New York: Marcel Dekker
- Brown KT, Flaming DG (1987) *Advanced micropipette techniques for cell physiology*. New York: John Wiley & Sons
- Burkoth TL, Bellhouse BJ, Hewson G, Longridge DJ, Muddle AG, Sarpie DF (1999) Transdermal and transmucosal powdered drug delivery. *Crit Rev Ther Drug Carrier Syst* 16:331-84
- Chabri F, Bouris K, Jones T, Barrow D, Hann A, Allender C et al. (2004) Microfabricated silicon microneedles for nonviral cutaneous gene delivery. *Br J Dermatol* 150:869-77

- Cormier M, Daddona PE (2003) Macroflux technology for transdermal delivery of therapeutic proteins and vaccines. In: *Modified-release drug delivery technology* (Rathbone MJ, Hadgraft J, Roberts MS, eds), New York: Marcel Dekker, 589-98
- Cormier M, Johnson B, Ameri M, Nyam K, Libiran L, Zhang DD et al. (2004) Transdermal delivery of desmopressin using a coated microneedle array patch system. *J Control Rel* 97:503-11
- Davis SP, Landis BJ, Adams ZH, Allen MG, Prausnitz MR (2004) Insertion of microneedles into skin: measurement and prediction of insertion force and needle fracture force. *J Biomech* 37:1155-63
- Davis SP, Martanto W, Allen MG, Prausnitz MR (2005) Transdermal insulin delivery to diabetic rats through microneedles. *IEEE Trans Biomed Eng* 52:909-15
- Gardeniers JGE, Lutge R, Berenschot JW, de Boer MJ, Yeshurun Y, Hefetz M et al. (2003) Silicon micromachined hollow microneedles for transdermal liquid transport. *J MEMS* 6:855-62
- Glenn GM, Kenney RT, Ellingsworth LR, Frech SA, Hammond SA, Zoetewij JP (2003) Transcutaneous immunization and immunostimulant strategies: capitalizing on the immunocompetence of the skin. *Expert Rev Vaccines* 2:253-67
- Haughton CL, Dillehay DL, Phillips LS (1999) Insulin replacement therapy for the rat model of streptozotocin-induced diabetes mellitus. *Lab Anim Sci* 49:639-44
- Kaushik S, Hord AH, Denson DD, McAllister DV, Smitra S, Allen MG et al. (2001) Lack of pain associated with microfabricated microneedles. *Anesth Analg* 92:502-4
- Lenhard MJ, Reeves GD (2001) Continuous subcutaneous insulin infusion: a comprehensive review of insulin pump therapy. *Arch Intern Med* 161:2293-300
- Lin W, Cormier M, Samiee A, Griffin A, Johnson B, Teng C et al. (2001) Transdermal delivery of antisense oligonucleotides with microprojection patch (Macroflux) technology. *Pharm Res* 18:1789-93
- Martanto W, Davis SP, Holiday NR, Wang J, Gill HS, Prausnitz MR (2004) Transdermal delivery of insulin using microneedles *in vivo*. *Pharm Res* 21:947-52
- Martanto W, Moore JS, Kashlan O, Kamath R, Wang PM, O' Neal JM et al. (2006) Microinfusion using hollow microneedles. *Pharm Res* 23:104-13
- Matriano JA, Cormier M, Johnson J, Young WA, BATTERY M, Nyam K et al. (2002) Macroflux microprojection array patch technology: a new and efficient approach for intracutaneous immunization. *Pharm Res* 19:63-70
- McAllister DV, Allen MG, Prausnitz MR (2000) Microfabricated microneedles for gene and drug delivery. *Annu Rev Biomed Eng* 2:289-313
- McAllister DV, Wang PM, Davis SP, Park J-H, Canatella PJ, Allen MG et al. (2003) Microfabricated needles for transdermal delivery of macromolecules and nanoparticles: fabrication methods and transport studies. *Proc Natl Acad Sci USA* 100:13755-60
- McGuire S, Yuan F (2001) Quantitative analysis of intratumoral infusion of color molecules. *Am J Physiol Heart Circ Physiol* 281:H715-21
- Miksza JA, Alarcon JB, Brittingham JM, Sutter DE, Pettis RJ, Harvey NG (2002) Improved genetic immunization via micromechanical disruption of skin-barrier function and targeted epidermal delivery. *Nat Med* 8:415-9
- Miksza JA, Sullivan VJ, Dean C, Waterston AM, Alarcon JB, Dekker JP et al. (2005) Protective immunization against inhalational anthrax: a comparison of minimally invasive delivery platforms. *J Infect Dis* 191:278-88
- Park J-H, Allen MG, Prausnitz MR (2005) Biodegradable polymer microneedles: fabrication, mechanics and transdermal drug delivery. *J Control Rel* 104:51-66
- Prausnitz MR (2004) Microneedles for transdermal drug delivery. *Adv Drug Deliv Rev* 56:581-7
- Prausnitz MR, Mitragotri S, Langer R (2004) Current status and future potential of transdermal drug delivery. *Nat Rev Drug Discov* 3:115-24
- Reed ML, Lye W-K (2004) Microsystems for drug and gene delivery. *Proc IEEE* 92:56-75
- Yang M, Zahn JD (2004) Microneedle insertion force reduction using vibratory actuation. *Biomed Microdev* 6:177-82